Journal of Physics: Conference Series

Analysis and performance assessment of the use of ammonia-based nano additive for lean combustion

Analysis and performance assessment of the use of ammonia-based nano additive for lean combustion

P Di Gloria[1], L Strafella[1], M G De Giorgi[1], G Ciccarella[2], G G Castelluzzo[2], F Baldassarre[2] and A Ficarella[1]

[1] Dep. of Engineering for Innovation, University of Salento, via per Monteroni, Lecce, I-73100, Italy
[2] Dep. of Science and Biological Technology and Environmental, University of Salento and CNR-Nanotec, via per Monteroni, Lecce, I-73100, Italy

Abstract. In recent years, considerable progress has been made in exploring new applications of fuel additives to reduce emissions. Reduction of total nitrogen oxide (NOx) emissions can be achieved by decreasing the flame temperature by using fuel emulsified with water and/or using ammonia-based nano additives such as urea. The use of water as part of the hydrocarbon fuel is also one of the prospective directions in the development of new types of fuel systems. For the preparation of emulsified fuel, it is desirable to achieve greater stability of the emulsified fuel with minimum expenditure of chemicals and energy, so that the emulsified fuel can be used for a longer period. The paper analyzed the influence of nano-dispersed urea particles, water, and surfactant (Span 80/ Tween 80) on the combustion stability and emission characteristics of aviation fuel. The experimental campaign was conducted on a test stand (a 300kW liquid vortex combustor of 300 kW) consisting of a cylindrical combustion chamber with four optical windows and equipped with high-precision pressure sensors, thermocouples, and an exhaust gas analyzer for acquiring emissions. The experimental campaign was conducted at a constant fuel/air ratio (Φ). One of the main focus is related to the stability of the emulsion. Chemiluminescence imaging was performed to characterize the effects of the additive on flame emissions. In addition, a statistical and spectral analysis was performed using the pressure sensor for instability analysis. Exhaust gas analysis was performed both with the additive described above and without additive for a constant Φ condition. The analysis was performed for NOx, carbon monoxide (CO) and carbon dioxide (CO_2) and oxygen (O_2).

1. Introduction

Modern aircraft engines must seek to increase the reduction of nitrogen oxide (NOx) emissions. At the present, the most easily applicable approach is to reduce the combustion temperature using 'cold flames' [1], because high temperature is the main reason for the formation of thermal NOx. The disadvantage of this approach is the loss of combustion efficiency.

Moving to lean conditions, i.e. reducing the fuel/air ratio, results in cold flames; but lowering the flame temperature increases the likelihood of the occurrence of flame instability, which could lead to extinguishing [2-4]. Irrespective of possible flame extinguishing, lean flames are subject to non-uniform mixing and the formation of hot spots can occur, which increases NOx production.

Another way to obtain cold flames is to use alternative fuels. Since this approach is more suitable for gas turbine engines, the addition of water to the fuel has been proposed to control combustion. The advantage of emulsified fuels is to influence the at atomization and evaporation of the fuel, which modifies pollutant emissions.

Atomizing diesel with water in the combustion chamber was studied by Wang et al. [5] using different ambient oxygen concentrations. By visualizing the flame, they observed that the fuel/air mixture was favored by micro-explosions in combination with the lowering of temperatures using water. For the same reason, soot emissions in diesel also decreased. Maawa et al. [6] studied how the use of water-emulsified diesel fuels affects performance, engine combustion characteristics, and exhaust emissions. The 30% water content by weight in the blended fuel reduced NOx emissions by approximately 26% compared to pure diesel fuel. Shen et al. [7] analyzed numerically how the atomization process of a water-oil spray is improved. They observed that the coalescence and diffusion of small water droplets dispersed in the oil during heating improved evaporation. Wang et al. [8] investigated that a combination of micro-explosion phenomena could stop soot emission in Diesels emulsified with water.

The main problem with water-emulsified fuels is the stability of the emulsion itself [9-11]. Sangki et al [12] studied how surfactants could avoid separation phenomena. They observed how different surfactants in water-emulsified diesel fuels impact combustion stability and engine performance. The surfactant that showed the best results was polyglyceryl-4-oleate, concluding that it could be used in real diesel engines. Melo-Espinoza et al. [13] performed an experimental study correlating diesel emulsion droplet size, water droplet size and its relationship with the occurrence of puffing and micro-explosion phenomena. These problems were studied using the surfactant sorbitan sesquioleate. Micro-explosions were only visualized in emulsions without surfactant while increasing the water ratio led to the formation of puffing. Bo-Jhih et al. [14] confirmed that the use of a surfactant increases the cost of emulsified fuels due to processing and material. To overcome this additional cost is to use emulsion fuels without the presence of surfactant [15], where a mixing system is required. The absence of surfactants in emulsified fuels leads to a mitigation of metal corrosion due to the acidity of surfactants [16].

Several studies have been carried out on the direct injection of water into the combustion chamber of gas turbine engines to reduce NOx emissions. however, high combustion efficiency losses have been observed due to the high-water content compared to the fuel [17, 18]. In contrast, fuels emulsified with water have shown more promising results. Indeed, Baena-Zambrana et al [19] through a literature review, studied the effect of different types of water-contaminated fuel and different operating conditions. Lean combustion of paraffin emulsified with water was investigated by Pourhoseini et al. [20], observing faster mixing, presence of micro-explosion of small emulsified fuel droplets; radiation heat flux and mean emissivity coefficient increased due to fuel emulsification, and lower flame temperature increased hydroxyl radicals (OH*), but a reduction in NOx. In addition, unburned hydrocarbons (UHC) were reduced compared to fuel that was not emulsified with water.

To further reduce NOx, urea may be added in liquid form to fuels emulsified with water. The thermal decomposition of the urea combustion process is described through equations (1) and (2) [21,22]:

$$(NH_2)_2CO \rightarrow NH_3 + HNCO \quad (1)$$

$$HNCO + H_2O \rightarrow NH_3 + CO_2 \quad (2)$$

In the presence of a flame, the following decomposition can be considered (3):

$$(NH_2)_2CO + H_2O \rightarrow 2NH_3 + CO_2 \quad (3)$$

where 1 mol of urea would generate 2 mol of ammonia.

The advantage of adding urea to the emulsion is the formation of ammonia that acts as a NOx reducing agent (Eqs. (4)-(7)):

$$4NH_3 + 4NO + O_2 \rightarrow 4N_2 + 6H_2O \quad (4)$$

$$4NH_3 + 6NO \rightarrow 5N_2 + 6H_2O \quad (5)$$

$$8NH_3 + 6NO_2 \rightarrow 7N_2 + 12H_2O \quad (6)$$

$$4NH_3 + 2NO_2 + 2NO \rightarrow 4N_2 + 6H_2O \quad (7)$$

In the past, gas turbine engines burning nitrogen compounds (NH3) have been studied, achieving an unacceptably low combustion efficiency and, therefore, research has been abandoned [23, 24].

The combustion of ammonia in air is difficult due to the low combustion heat, the self-ignition temperature, a narrow flammability range and the high degree of toxicity. However, it has recently been shown that stable combustion of ammonia can be achieved by using turbine burners, thus stimulating the interest of the lost research [25]. The gaseous nature of ammonia leads to a modification of the

turbine, such as the supply system, pressure regulators, compressors, etc. that increases the degree of complexity of the aircraft. But a source of solid ammonia can be dispersed in the fuel [26] and thus be used without modifying the aircraft installation. In addition, urea is stable and can be burned without compromising the stability of the flame.
Experimentally, Mosevitzky et al. [27] investigated the effects of the water content when igniting aqueous ammonia/ammonium nitrate and urea/ammonium nitrate fuels. The self-ignition temperature is increased in the presence of water.
The literature does not propose work with Jet-A1 emulsified with water and urea applied to aircraft engines to control combustion. The problem of flame stability, which is related to pollutant emissions from real aircraft engines, deserves in-depth study. The most important advantage of emulsified fuel is that it does not completely modify the aircraft engine, but, at most, only an upgrade. The stability of the emulsion is a drawback to be considered, which, however, could be overcome by the use of surfactants. The risk of ice is another problem to be concerned with, due to the presence of water and urea in the fuel emulsion; aircraft should be equipped with anti-icing systems (e.g., using additives) due to very cold external conditions, such as very high altitudes.
The impact of water was further investigated by De Giorgi et al. and Fontanarosa et al. [28-29]. The authors showed a beneficial effect of water in the emulsion, registering a reduction in NOx when operating under lean combustion conditions ($\Phi = 0.36$), but more unstable flame dynamics and worse performance under ultra-lean conditions ($\Phi < 0.36$).
Using lean combustion in a 300-kW liquid-fuelled vortex combustion chamber, this work provides an experimental investigation into the effects of water-urea emulsion in Jet-A1 with and without surfactants.
The stoichiometric coefficient Φ was set at 0.24 and the weight percentages of the emulsion phases are 2.03 wt% urea, 2.54 wt% water and 6.54 wt% surfactant.
The impact of the two different emulsions in terms of reducing emissions of NOx, oxygen (O_2), carbon monoxide (CO) and carbon dioxide (CO_2) was assessed. flame stability was studied by installing a pressure sensor and analyzing its frequency content, statistical via root mean square (RMS), and spectral via the second moment as an indicator of combustion stability. Using chemiluminescence emission images of the hydroxyl radical (OH), methylidene (CH), amino (NH_2) and imidogen (NH) by equipping the test bench with a high-speed ICCD.
In summary, the novelty of the following work can be listed as follows:
- investigation of the effect of surfactant in the aqueous-urea emulsion in Jet-A1 to control its stability and to decrease pollutant emissions,
- the study of flame instability through chemiluminescence images of CH*, OH*, NH*, NH_2*;
- analysis of the pressure inside the combustion chamber through the frequency domain, through statistical methods for the stability assessment of emulsified fuel flames with and without surfactant.

2. Materials and methods

2.1 Emulsion preparation in Jet-A1

The first emulsion of water and urea in Jet-A1 emulsion and the second emulsion equal to the first but with the addition of surfactants were prepared by the Institute of Nanotechnology (NANOTEC) in Lecce (Italy).
Water, solid urea, and surfactants were added to a special tank containing Jet-A1 fuel. Using the UltraTurrax T25, the emulsion was homogenized for at least 5 minutes. During the experimental tests, the homogeneity of the water-urea emulsion in Jet-A1 was ensured by providing continuous agitation with UltraTurrax T25, whereas the water-urea-surfactant emulsion in Jet-A1 did not require continuous agitation due to its stability.
follow these instructions as carefully as possible so all articles within a conference have the same style to the title page. This paragraph follows a section title so it should not be indented.

2.2 Experimental apparatus, methodologies, and techniques

The experimental campaign was carried out at the University of Salento (Lecce, Italy) at the Green Engine laboratory. The test bench is derived from a gas turbine configuration for aircraft engines and,

specifically, is a 300 kW cylindrical liquid combustion chamber. It has a length of 29 cm and an inner diameter of 14 cm; two concentric annular tubes allow air to enter. Before entering the combustion chamber, a 45° eight-septa swirler is mounted on the inner tube. Figure 1(a) depicts a picture of the setup; for more details, the authors refer to De Giorgi et al. [28].
In the following work, the combustor was used in non-premixed mode. The total air injection, as can be seen in Figure 1(b) is composed of the contribution of the primary (axial) air flow entering the burner (blue path) and a secondary swirl air flow (red path). The liquid fuel line is represented by the green path to the axial spray injector, consisting of a Monarch 1.20 45° R single-hole nozzle with a 45° injection angle.

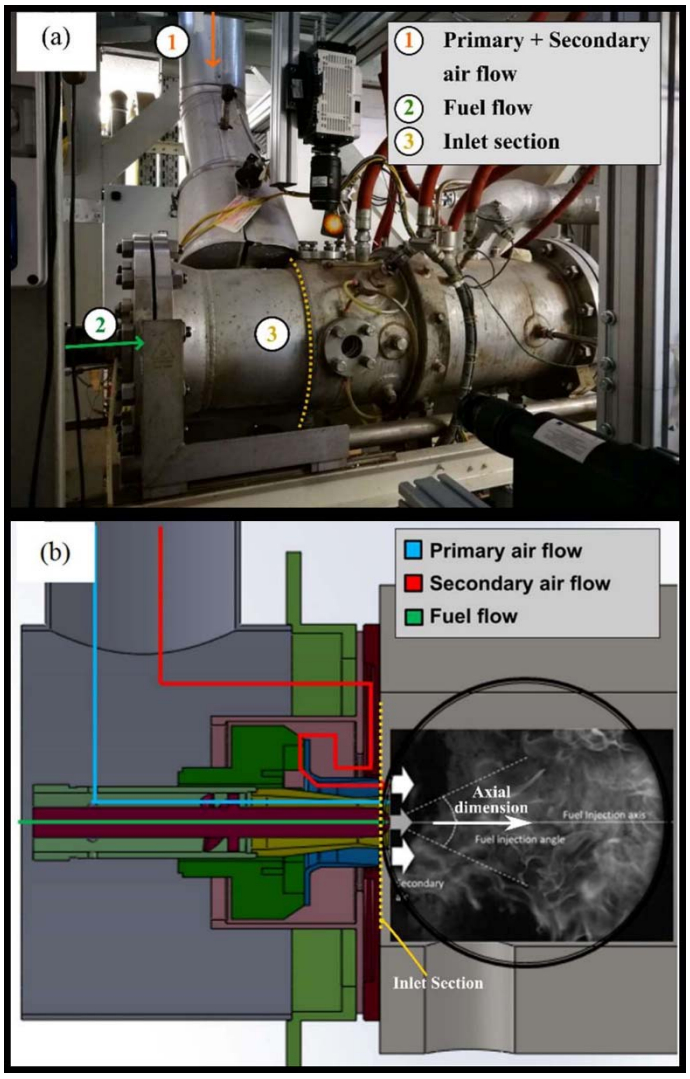

Figure 1. *Green Engine burner: (a) setup; (b) sketch of the setup in non-premixed combustion mode. (For interpretation of the references to color in this figure legend, the reader is referred to the web version of this article.)*

The most important information was recorded at a frequency of 4 Hz and with the LabVIEW® platform from National Instruments,: temperatures through T-type thermocouples, fuel mass flow through a VSE EF flow meter 0.04 ARO 14 V PNP/2 and air flow was measured with an Asa-C6-3100/38/EX1 flow meter. 1000 samples were averaged over the recorded signals.
The pressure inside the combustion chamber was acquired by placing the Kistler PiezoSmart pressure sensor type 4045A2 on the inside walls of the combèustion chamber in the combustion zone. The pressure sensor was coupled with the type 4618A0 piezoresistive amplifier with a pressure range of [0 to 2] bar, and pressure signals were recorded at a sampling rate of 10 kHz using a LabVIEW® control

and acquisition system from National Instruments. A cooling circuit installed around the pressure sensor kept the local temperature below its maximum operating temperature of 413 K.
Through the Horiba PG-350E model gas analyzer, at a sampling frequency of 1 Hz, exhaust gas emissions of NOx, CO, CO_2 and O_2 species were simultaneously acquired. The sensitivity of the instrument is 0.01% for CO_2 emissions and 1ppm for all other emissions.
High-speed flame images were recorded using the circular quartz windows installed in the combustion chamber. The instrumentation used is an intensified CCD camera (ICCD), consisting of the Phantom M320S camera coupled with a Lambert intensifier. The latter was equipped with a 78mm UV lens with an f/3.8 aperture and was coupled to several interchangeable narrow-band filters: one for the chemiluminescence emission of the hydroxyl radical (OH*) with a central wavelength of 307 ± 10 nm, another with a wavelength of 436 ± 10 nm for the chemiluminescence emission of the methylidyne radical (CH*), the third filter with a wavelength of 336 ± 10 nm for the chemiluminescence emission of the imidogen radical (NH) and the last filter with a wavelength of 632 ± 10 nm for the chemiluminescence emission of the amino radical (NH_2). For imaging the chemiluminescence emission, OH* was intensified by a factor of 8, CH* and NH were intensified by a factor of 7 and NH2 was intensified by a factor of 4.5. For both tests, the number of images was set to 1000 and the flame images were recorded at 1000 Hz, with a resolution of 875 × 656 pixels.

2.3 Test matrix and conditions

The operating conditions of the experimental campaign are described below. The inlet air was preheated to 410 K for both test cases, the emulsions were injected at 7 bar using an AUDI 8K0.906.095.B Pierburg 7.50103.00 pump. The experiments carried out in this test campaign are summarised in Table 1. The equivalence ratio Φ was kept constant for all tests based on the stoichiometric air-fuel ratio of paraffin which is defined as $\Phi = \left(\frac{\dot{m}_f}{\dot{m}_a}\right) \Big/ \left(\frac{\dot{m}_f}{\dot{m}_a}\right)_{st}$ where $\dot{m}$ is the mass flow rate and the subscripts *f* and *a* refer to the fuel and the air flows, and and st denotes the stoichiometric conditions. The value of Φ was set at 0.24. The contents of urea, water and surfactants are expressed as a percentage mass fraction wt%, i.e. the percentage ratio between the mass of the substance and the mass of the emulsified fuel. The density of each liquid phase composing the emulsion was estimated by averaging the volume fraction and considering the density of Jet-A1 of 780 kg/m^3, the density of water of 1000 kg/m^3, the density of urea of 1320 kg/m^3, the density of Span 80 of 1000 kg/m^3 and the density of Tween 80 of 1070 kg/m^3. It was found that the increase in density due to the water-urea-surfactant emulsion and water-urea emulsion is about 1% of the density of pure Jet-A1.

Table 1. Test matrix: test case, equivalence ratio and fuel compositions.

Test case	Φ (-)	H_2O (wt%)	Urea (wt%)	Mix Tween 80/Span 80 (wt%)	ρ_f (kg/m^3)
1	0.24	0	0	0	780
2	0.24	2.5	2	6.5	795
3	0.24	2.5	2	0	793

3 Results

The following section will be divided into the following subsections: subsection 3.1 will discuss the statistical analysis conducted for the data acquired via the pressure sensor positioned inside the burner combustion zone, then subsection 3.2 will analyze the frequency domain of the data acquired with the pressure sensor by exploiting the Fast Fourier Transform, subsection 3.3 where chemiluminescence emission images acquired through the ICCD Fast Fourier Transform will be taken into consideration, and finally, the last subsection 3.4 will investigate the pollutant emissions of NOx, CO_2, CO and O_2 to establish the effects of surfactants.

3.1 Statistical analysis of the pressure signal

The following subsection presents the data recorded through the pressure sensor that has been installed inside the burner in the combustion zone. For each test case, about 950000 pressure values were recorded (Figure 2) under 3 different fuel compositions: pure fuel, urea 2wt%+water 2.5wt% surfactants 6.5wt%

and urea 2wt% + water 2.5wt%. Figure 3 shows the probability distribution of the acquired pressure signal.
It should be underlined that these data were obtained very near the combustor's stability boundary. In fact, further changes in operating conditions resulted in the combustor becoming unstable.
Figure 3 shows that the shapes of all three PDFs are quite similar, although their mean amplitudes are different. Specifically, these PDFs are all symmetric and resemble Gaussian-type distributions
The more stable operating conditions (test 1 and 2) present peaks at a low amplitude(test 1: 1.0256 bar, test 2: 1.0249 bar), and remains in a narrow range of values and the distribution is quite symmetric. The probability distribution of the test 3 with urea and without surfactant, presents a peak at a slightly larger amplitude (test 3: 1.0288 bar) and is broader than the case without urea or with urea and surfactantm implying that the oscillations exhibit a wider range of amplitudes.
Through the considerations just made, statistically, the presence of surfactants in the fuel emulsion leads to less unstable combustion than without surfactant.

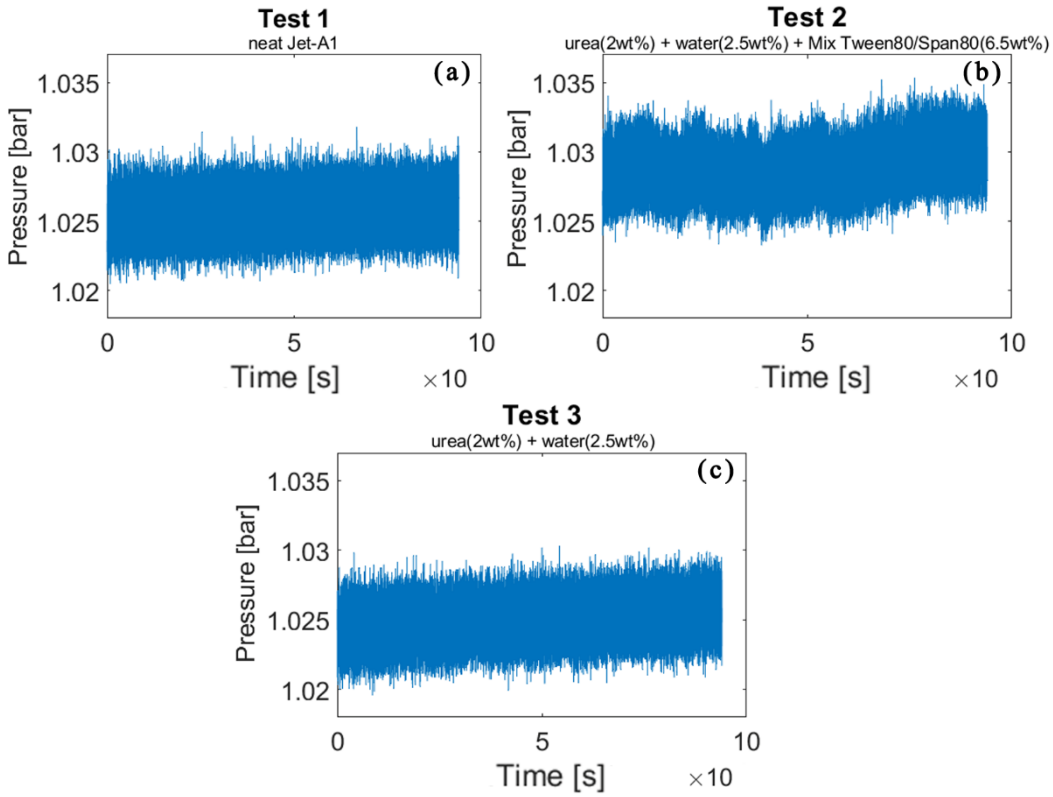

Figure 2. *Pressure signals acquired: (a) test 1 consisting of neat Jet-A1, (b) test 2 consisting of urea 2wt% + water 2.5wt% + surfactants 6.5wt%, (c) test 3 consisting of urea 2wt% + water 2.5wt%.*

3.2 Spectral analysis of the pressure signal

The spectral analysis of the signals recorded via the pressure sensor is based on the Fast Fourier Transform (Figure 4), thus moving from the time domain to the frequency domain. The signal was recorded with a sampling rate of 10 kHz and, consequently, the FFT study has a domain of up to 5 kHz. All tests show two characteristic peaks at almost equal frequencies, but test 3 (Figure 4 (c)) has smaller amplitudes than the other two tests. Moreover, test 3 has a frequency content, which the other two tests do not possess, around 3300 Hz. Through this frequency comparison, it is confirmed that the emulsion with surfactants is very similar to the case of pure Jet-A1, making combustion stable. In contrast, test 3 (Figure 4 (c)) has more unstable combustion.

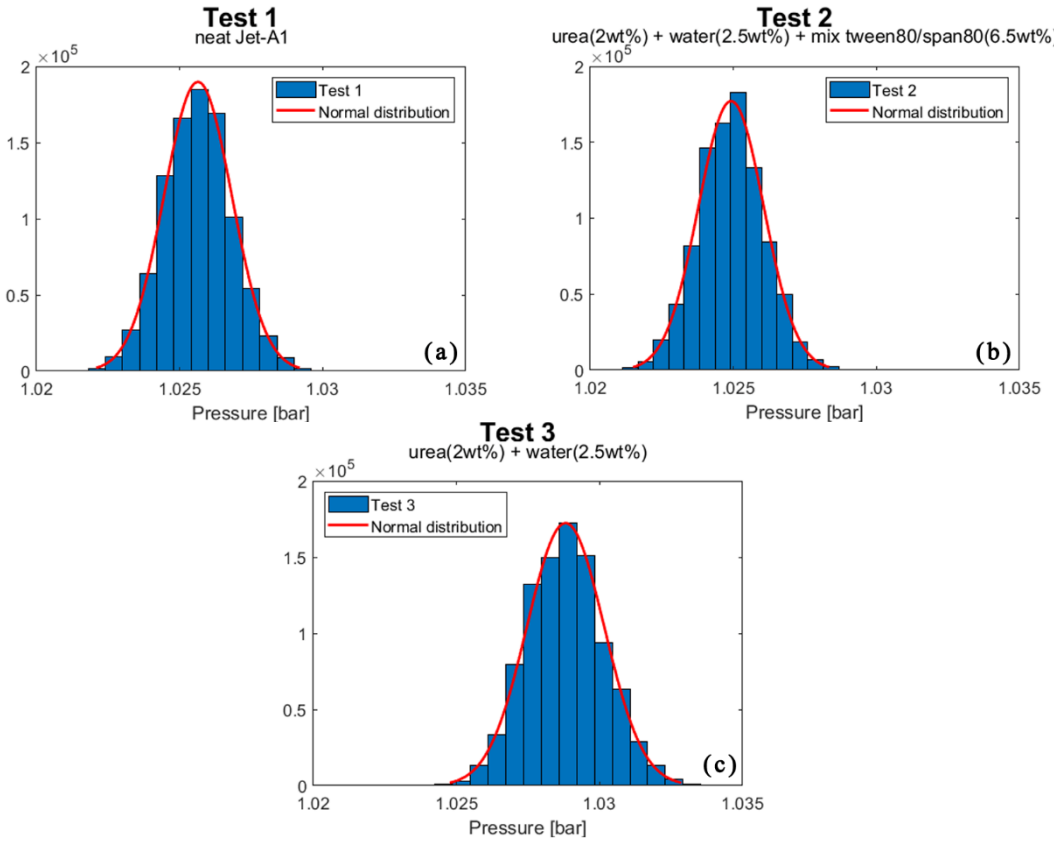

***Figure 3**. Distribution of the acquired pressure signal: (a) test 1 consisting of neat Jet-A1, (b) test 2 consisting of urea 2wt% + water 2.5wt% + surfactants 6.5wt%, (c) test 3 consisting of urea 2wt% + water 2.5wt%.*

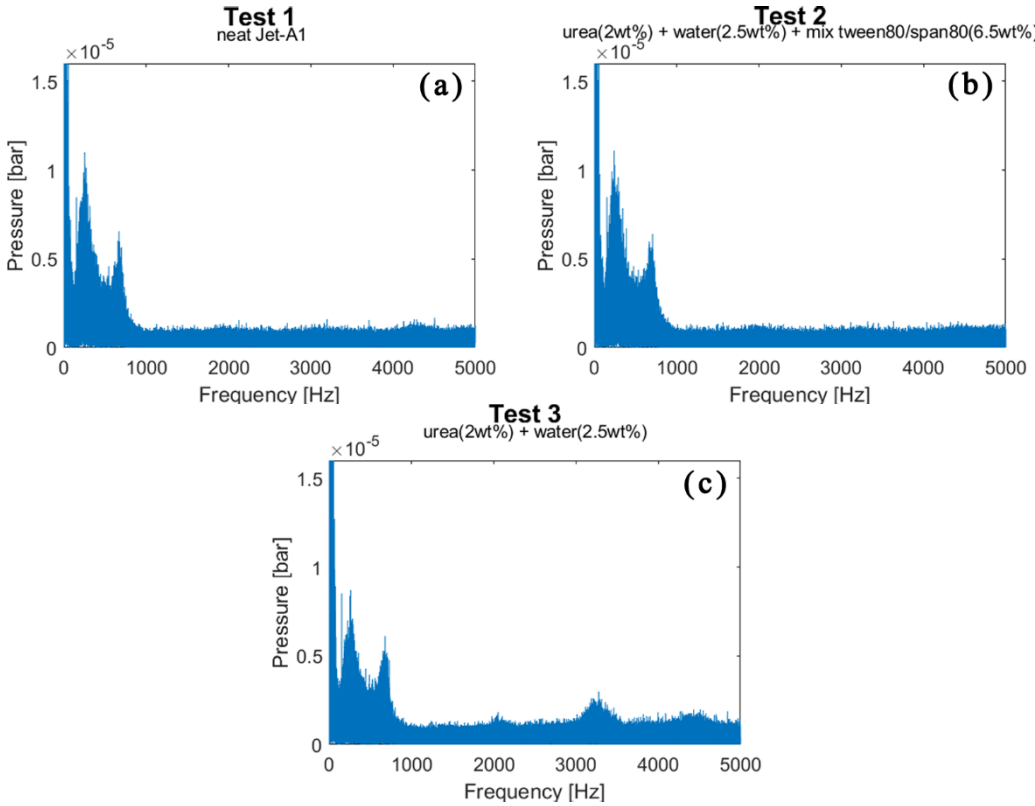

Figure 4. *Fast Fourier Transform of the acquired pressure signal: (a) test 1 consisting of neat Jet-A1, (b) test 2 consisting of urea 2wt% + water 2.5wt% + surfactants 6.5wt%, (c) test 3 consisting of urea 2wt% + water 2.5wt%.*

3.3 Chemiluminescence emissions

The chemiluminescence emission analysis was conducted at a constant stoichiometric coefficient Φ of 0.24. The circular optical quartz window is positioned so that the flame is visible at the height of the injector (in Figures 5-9, the spray cone is visible). The images acquired by the camera are the projection along the line of sight In this subsection, all chemiluminescence emission images are an average of 1000 frames captured in 1 second. Figure 5 shows the broadband UV chemiluminescence.

Both OH* and CH* radicals are produced in the reaction region, so the are with the maximum intensities are a good indicator of the flame front.

The flame shape is quite similar for the two test cases 1 and 2 while differs in the case with urea but without surfactant. Figure 6 shows the chemiluminescence emission of the hydroxyl radical OH* acquired using the bandpass filter with a wavelength centered at 307 ± 10nm . The OH* radical is an identifier of the combustion product, indeed in Figures (a), (b), (c) the shapes of the structures are similar even if there is a shift of the OH* emission area downstream of the nozzle exit away from the spray in presence of urea addition. Figure 7 was obtained using a bandpass filter with a wavelength centered at 436 ± 10nm for the chemiluminescence emission of the methylidene radical. The CH* radical is an excellent fuel identifier; in fact, the shape of the structures is different between the 3 tests; these differences depend on the composition of the emulsion.

Figure 7 (b) recorded a spatially more homogeneous light intensity than Figure 7 (c), no doubt due to the presence of the surfactants stabilizing the emulsion. Figure 8 and Figure 9 missing test 1 (i.e. neat Jet-A1); this is because the filters used (NH* and NH_2) are predominantly for the observation of ammonia formation.

The primary oxidation pathway of NH_3 includes reactions:

$$NH_3 + H = NH_2 + H_2 \quad (8)$$

$$NH_3 + OH = NH_2 + H_2O \quad (9)$$

NH_3 is mainly consumed through H-abstraction reactions by H and OH to form NH_2 radical, then NH_2 radical can further react with H and OH to form NH radical.
The secondary oxidation reaction of NH_2 to NH (see Fig. 16) also proceeds mainly through the H-abstraction reactions via H and OH.

$$NH_2 + H = NH + H_2 \quad (10)$$

$$NH_2 + OH = NH + H_2O \quad (11)$$

Figures 8 and 9 show that the major products and key intermediates are different without and with the surfactant.
Figure 8 reports the time-average NH* images acquired using a bandpass filter with a wavelength centered in 336 ± 10nm for the chemiluminescence emission of the imidogen radical.
While Figure 9 was obtained using a bandpass filter with a wavelength centered in 632 ± 10nm for the chemiluminescence emission of the amino radical.
The decomposition of ammonia to NH, NH_2, and N in the case without surfactant has been significantly enhanced. The NH* and NH_2* present stronger chemiluminescence signal intensity in Test Case 3.
in Figures 8(a) and 8(b) the shape of the area at high NH* emission are similar even this area is wider for the test 3.
The region with strong NH* chemiluminescence signals fully coincides with the flame shape illustrated in Figure 6.
The region with strongest NH_2* chemiluminescence signals is observed from the top view and close to the nozzle exit. The signal intensity for Test case 3 is remarkably higher than that for Test case 2.
The shape of the spatial structure in Figure 9(a) is influenced by the presence of the surfactants and, unlike in Figure 9(b), the surfactants reduce the formation of NH_2.

3.4 Pollutant emissions
In this last subsection, the emission of pollutant gases is studied. It should be noted that the stoichiometric coefficient is constant for all tests, equal to 0.24.

Considering Figure 10 (a), test 2 presents a higher NOx emission than the neat Jet-A1, test 3 presents slightly higher emissions than the neat Jet-A1 case.

The presence of surfactants (test 2), have a negative effect on NOx of about 3 times as much as the case without them (test 3).

As evidenced by the NH2* chemiluminescence, the central high-temperature, ammonia-rich flame facilitates an extensive formation of NH2*.

The possible reactions associated with NO reduction include

$$NO + NH_2 = NNH + OH \quad (12)$$

$$NO + NH_2 = N_2 + H_2O \quad (13)$$

So the test case 3 with higher NH_2* emissions than test case 2, presents lower NO.

Figure 10 (b) shows that, again, the presence of surfactants increases also CO emission compared to test 3 (urea + water) and test 1 (neat Jet-A1). Figure 10 (c) shows how the surfactants significantly reduce CO_2 emission compared to test 1 and 3, whereas test 3 only slightly increases carbon dioxide emission

compared to the pure Jet-A1 case. The last figure 10 (d) shows a high presence of O_2 in the exhaust gas for test 2, indicating incomplete combustion.

4 Conclusions

This paper presents the results of an investigation on the effect of the presence or absence of surfactants within an emulsion consisting of urea and water on flame stability and exhaust gas emission on a 300-kW liquid-fuelled swirling combustor for a lean combustion condition. The conclusions of this study can be summarised as follows:

- by analyzing the statistical distribution and spectral analysis of the data acquired via the pressure sensor, it is shown that the presence of surfactants in the urea-water emulsion is very similar to the case of neat Jet-A1, as well as improving the stability of the emulsion itself;
- the study of the average chemiluminescence emission images showed that the OH* hydroxyl radical is an excellent element for studying the quality of the combustion product, the CH* methylidine radical is a fuel identifier, while the NH* imidogen and NH_2* amino radicals are an excellent tool for visualizing and understanding the decomposition of ammonia within combustion and possible effects on NO_x formation;

- the increase in NH* imidogen and NH_2* amino radicals intensities is much lower in presence of surfactant;

- the pollutant emissions were investigated to show that, although surfactants have a positive effect on emulsion and flame stability, the presence of surfactants has a worsening effect on pollution at the stoichiometric coefficient investigated ($\Phi = 0.24$).

Future work will be an experimental investigation of the effect of surfactants on ultra-lean and richer flames.

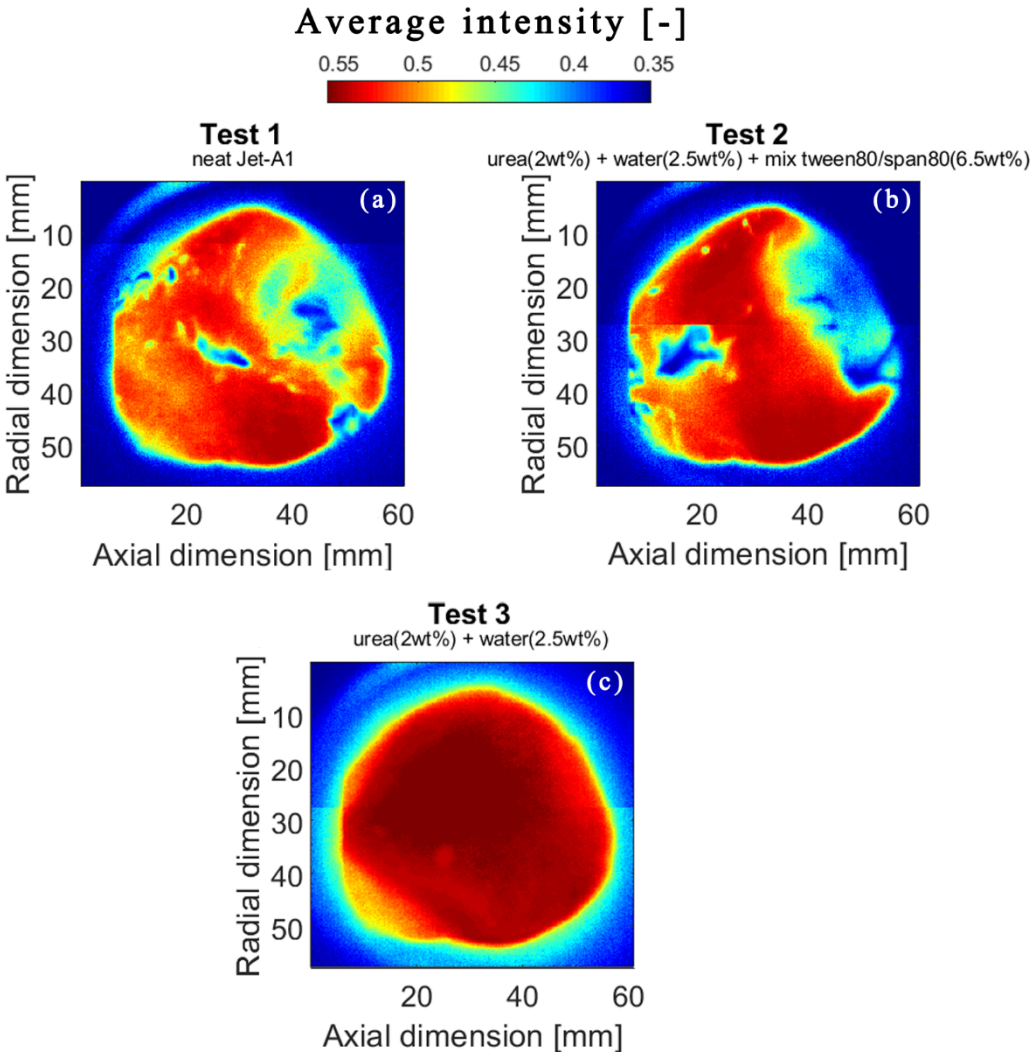

Figure 5. *Average images of broadband chemiluminescence: (a) test 1 consisting of neat Jet-A1, (b) test 2 consisting of urea 2wt% + water 2.5wt% + surfactants 6.5wt%, (c) test 3 consisting of urea 2wt% + water 2.5wt% at Φ = 0.24.*

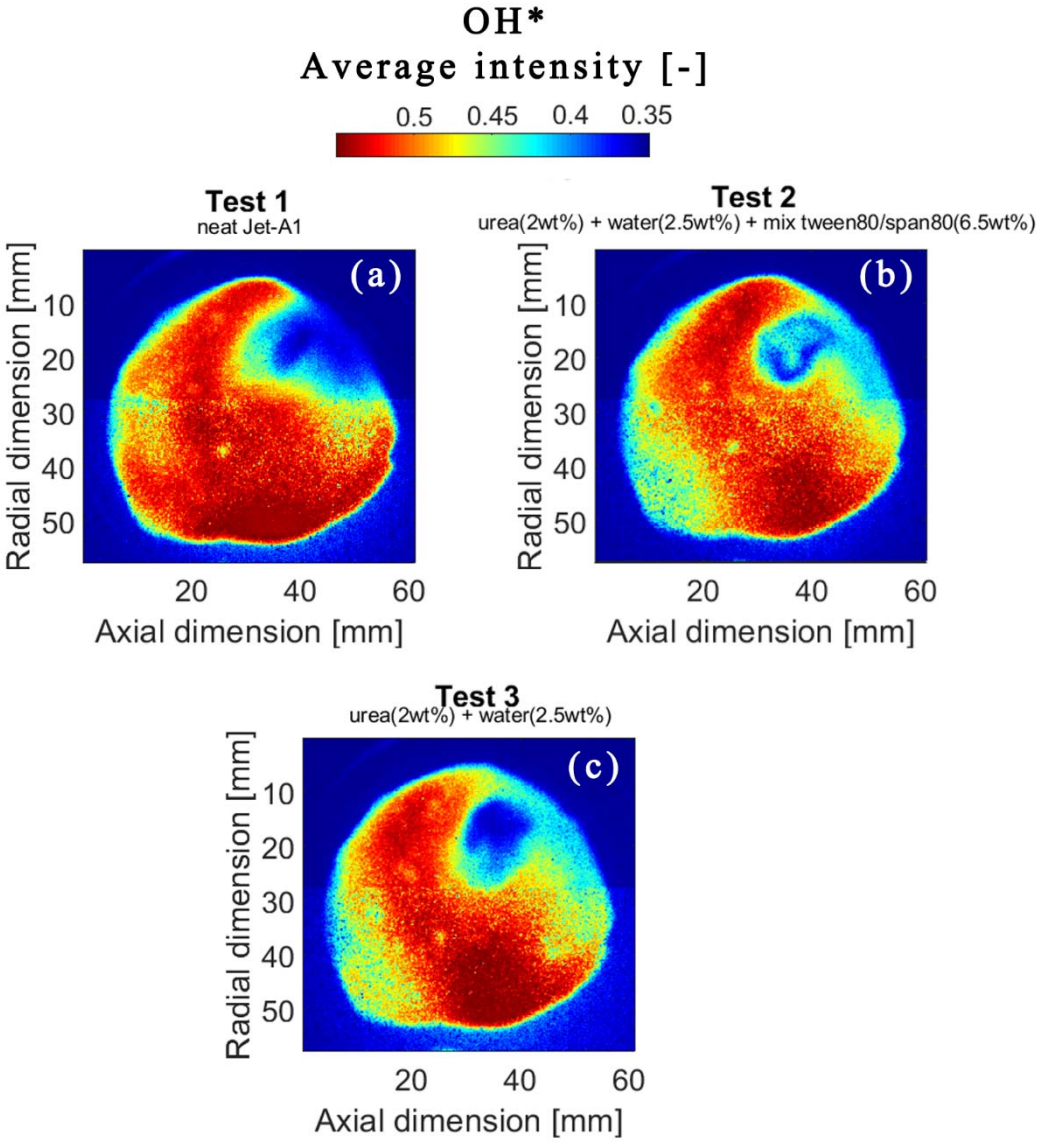

***Figure 6**. Average images of the OH* chemiluminescence emission: (a) test 1 consisting of neat Jet-A1, (b) test 2 consisting of urea 2wt% + water 2.5wt% + surfactants 6.5wt%, (c) test 3 consisting of urea 2wt% + water 2.5wt% at $\Phi = 0.24$.*

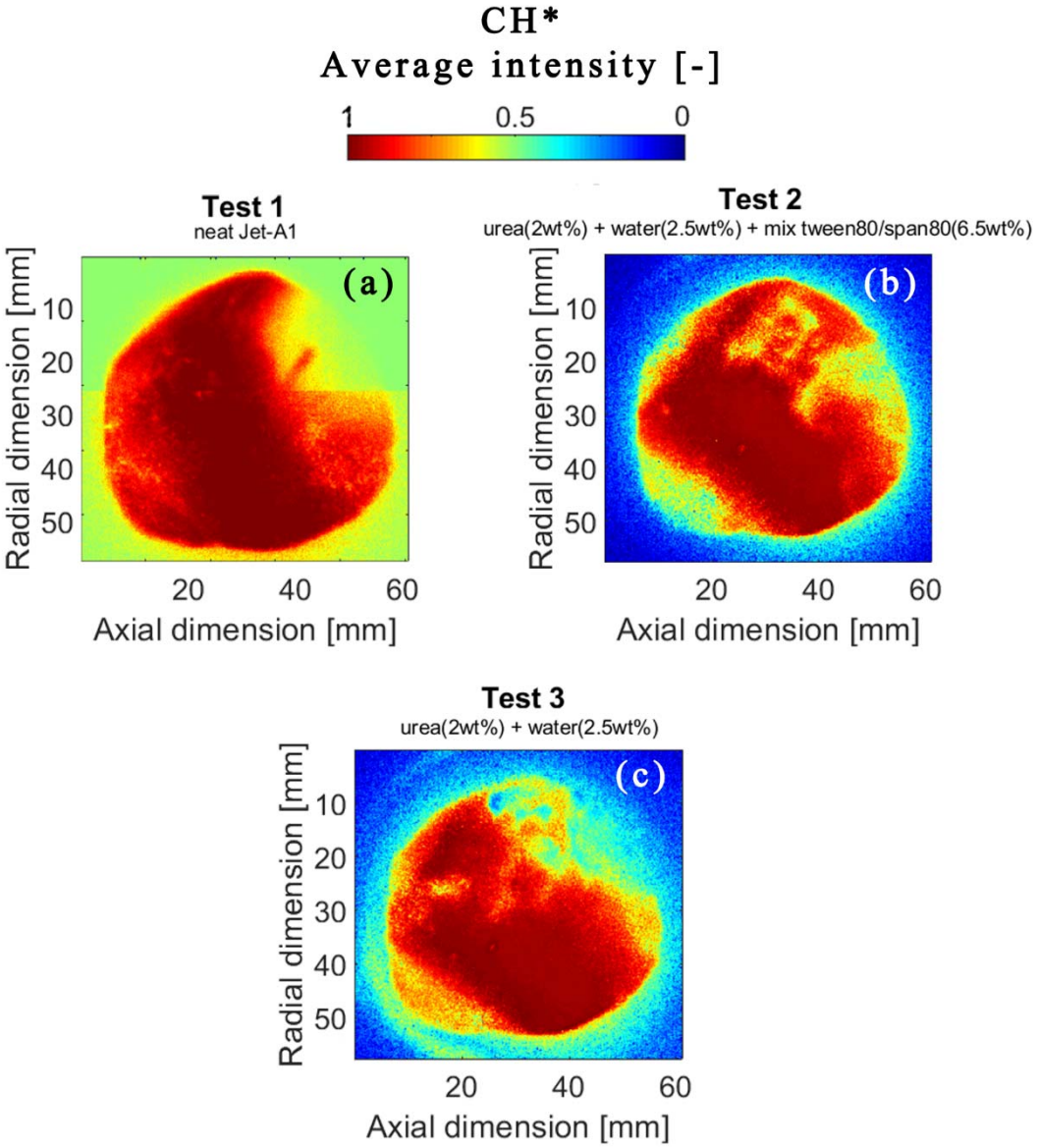

Figure 7. *Average images of the CH* chemiluminescence emission: (a) test 1 consisting of neat Jet-A1, (b) test 2 consisting of urea 2wt% + water 2.5wt% + surfactants 6.5wt%, (c) test 3 consisting of urea 2wt% + water 2.5wt% at* $\Phi = 0.24$.

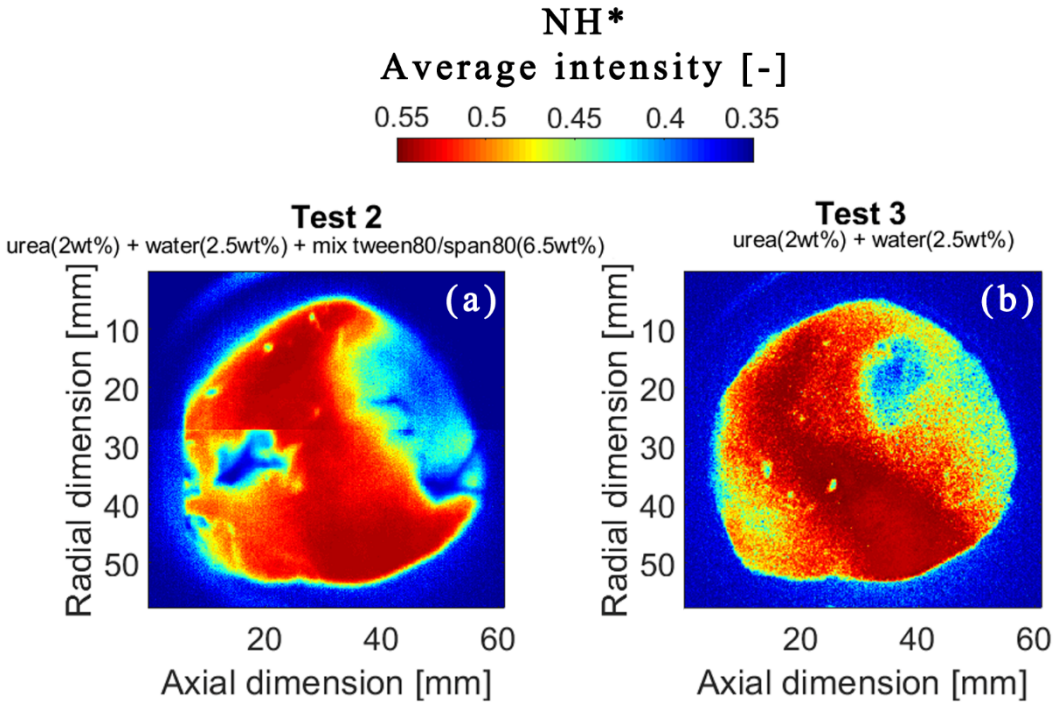

Figure. 8. *Average images of the NH* chemiluminescence emission: (a) test 1 consisting of neat Jet-A1, (b) test 2 consisting of urea 2wt% + water 2.5wt% + surfactants 6.5wt%, (c) test 3 consisting of urea 2wt% + water 2.5wt% at Φ = 0.24.*

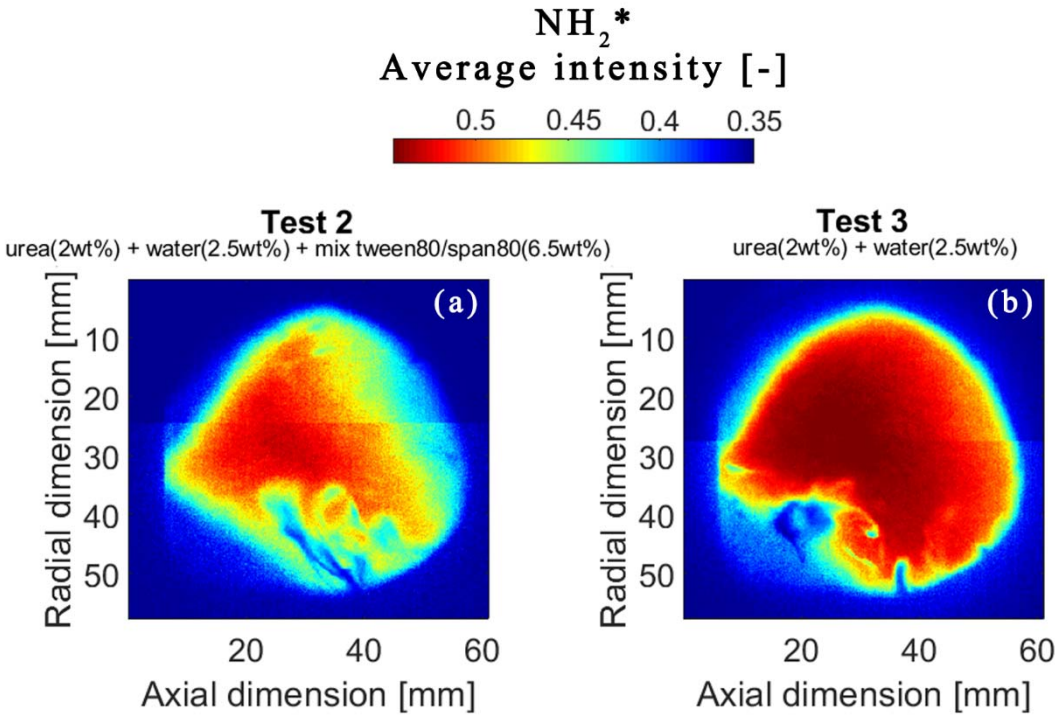

Figure 9. *Average images of the NH_2* chemiluminescence emission: (a) test 1 consisting of neat Jet-A1, (b) test 2 consisting of urea 2wt% + water 2.5wt% + surfactants 6.5wt%, (c) test 3 consisting of urea 2wt% + water 2.5wt% at Φ = 0.24.*

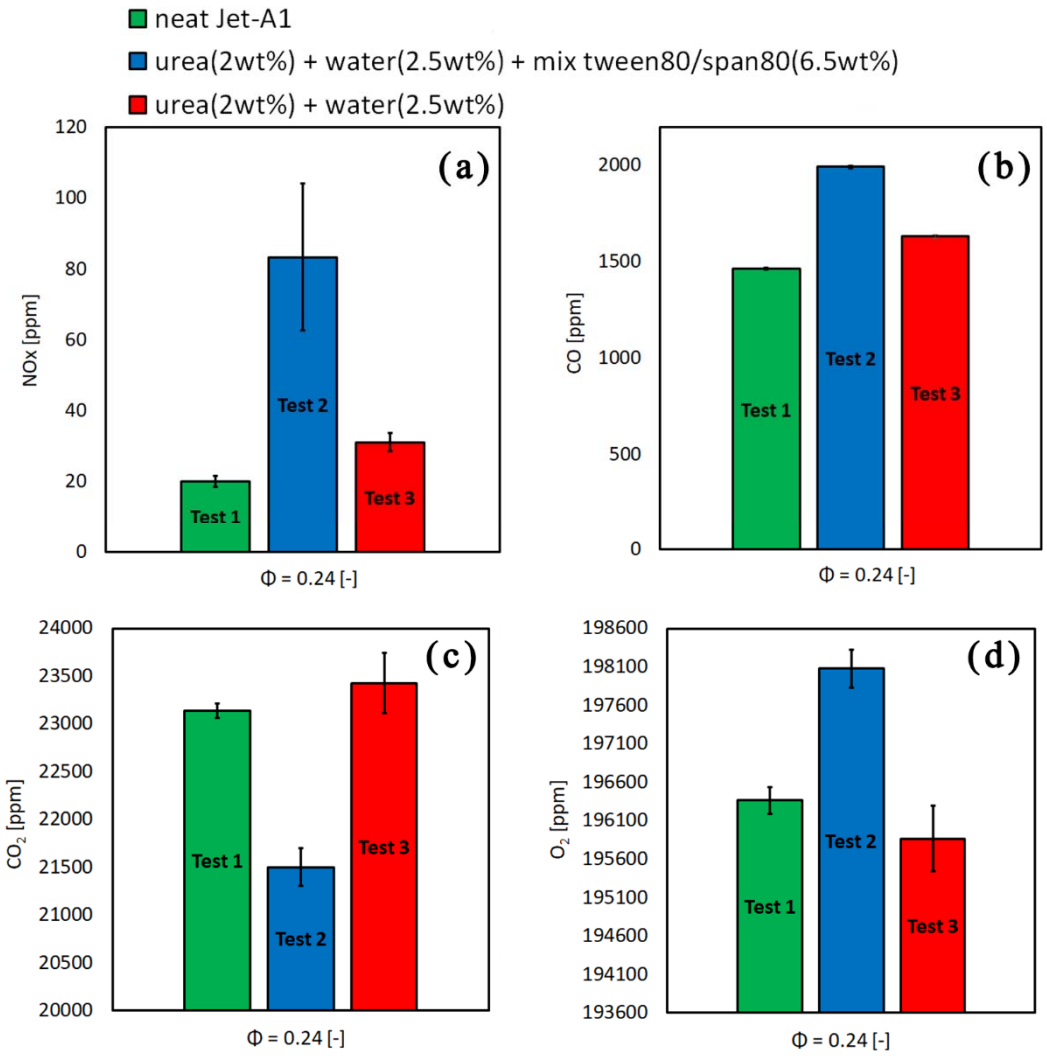

***Figure 10**. Pollutant emission for each test: (a) NOx ppm, (b) CO ppm, (c) CO_2, (d) O_2 at $\Phi = 0.24$.*

Acknowledgments

The work was supported and funded by the PON R&I 2014–2020 Asse I "Investimenti in Capitale Umano" Azione IV.5 "Dottorati Innovativi sulle tematiche Green" - Corso di Dottorato in "Ingegneria dei Sistemi Complessi" XXXVII ciclo - Università del Salento".

References

[1] Lindstrom B, Karlsson JAJ, Ekdunge P, De Verdier L, Haggendal B, Dawody J, et al. *Diesel fuel reformer for automotive fuel cell applications*. Int J Hydrogen Energy 2009; 34(8):3367–81.

[2] De Giorgi MG, Sciolti A, Campilongo S, Ficarella A. *Image processing for the characterization of flame stability in a non-premixed liquid fuel burner near lean blowout*. Aerospace Science and Technology 2016; 49:41–51. https://doi.org/10.1016/j.ast.2015.11.030.

[3] Kaluri A, Malte P, Novosselov Igor. *Real-time prediction of lean blowout using chemical reactor network*. Fuel 2018; 234:797–808. https://doi.org/10.1016/j.fuel.2018.07.065.

[4] De Giorgi MG, Campilongo S, Ficarella A, De Falco G, Commodo M, D'Anna A. *Pollutant formation during the occurrence of flame instabilities under very-lean combustion conditions in a liquid-fuel burner*. Energies 2017;10(3):352. https://doi.org/10.3390/en10030352.

[5] Wang Z, Wu S, Huang Y, Huang S, Shi S, Cheng X, et al. *Experimental investigation on spray, evaporation and combustion characteristics of ethanol-diesel, water emulsified diesel and neat diesel fuels*. Fuel 2018; 231:438–48. https://doi.org/10.1016/j.fuel.2018.05.129.
[6] Maawa WN, Mamat R, Najafi G, De Goey LPH. *Performance, combustion, and emission characteristics of a CI engine fueled with emulsified diesel-biodiesel blends at different water contents*. Fuel 2020; 267:117265. https://doi.org/10.1016/j.fuel.2020.117265.
[7] Shen S, Che Z, Wang T, Yue Z, Sun K, Som S. *A model for droplet heating and evaporation of water-in-oil emulsified fuel*. Fuel 2020; 266:116710. https://doi.org/10.1016/j.fuel.2019.116710.
[8] Wang Z, Chen X, Huang S, Chen Y, Mack JH, Tang J, et al. *Visualization study for the effects of oxygen concentration on combustion characteristics of water emulsified diesel*. Fuel 2016; 177:226–34. https://doi.org/10.1016/j.fuel.2016.03.010.
[9] L Daggett DL, Ortanderl S, Eames D, Berton JJ, Snyder CA. *Revisiting water injection for commercial aircraft*. In: Session: Turbine Engine Technologies, 2004, November.
[10] Francioso L, De Pascali C, Sglavo V, Grazioli A, Masieri M, Siciliano P. *Modelling, fabrication and experimental testing of an heat sink free wearable thermoelectric generator*. Energy Convers Manag 2017; 145:204–213. ISSN 0196-8904. https://doi.org/10.1016/j.enconman.2017.04.096.
[11] Ghannam MT, Selim MYE. *Stability behavior of water-in-diesel fuel emulsion Pet*. Sci Technol 2009; 27(4):396–411. https://doi.org/10.1080/10916460701783969.
[12] Park S, Woo S, Kim H, Lee K. *The characteristic of spray using diesel water emulsified fuel in a diesel engine*. Appl Energy 2016; 176:209–20.
[13] Melo-Espinosa EA, Bellettre J, Tarlet D, Montillet A, Piloto-Rodríguez R, Verhelst S. *Experimental investigation of emulsified fuels produced with a micro-channel emulsifier: puffing and micro-explosion analyses*. Fuel 2018; 219:320–30. https://doi.org/10.1016/j.fuel.2018.01.103.
[14] Lin B-J, Chen W-H, Budzianowski WM, Hsieh C-T, Lin P-H. *Emulsification analysis of bio-oil and diesel under various combinations of emulsifiers*. Appl Energy 2016; 178:746–57.
[15] Nurul Aiyshah Mazlan, Wira Jazair Yahya, Ahmad Muhsin Ithnin, Hasannuddin AK, Nur Atiqah Ramlan, Dhani Avianto Sugeng, Muhammad Adib AR, Tsuyoshi Koga, Rizalman Mamat, Nor Azwadi Che Sidik. *Effects of different water percentages in non-surfactant emulsion fuel on performance and exhaust emissions of a light-duty truck*. J Clean Prod 2018; 179:559–566. https://doi.org/10.1016/j.jclepro.2018.01.143.
[16] Chandran D, Khalid M, Raviadaran R, Lau HLN, Yung Chee Liang, Kanesan Dinesh, Salim Mohammed. *Sustainability of water in diesel emulsion fuel: an assessment of its corrosion behaviour towards copper*. J Cleaner Prod 2019; 220:1005–13. https://doi.org/10.1016/j.jclepro.2019.02.210.
[17] Farokhipour, Hamidpour E, Amani E. *A numerical study of NOx reduction by water spray injection in gas turbine combustion chambers*. Fuel 2018; 212:173–86. https://doi.org/10.1016/j.fuel.2017.10.033.
[18] Pugh DG, Bowen PJ, Marsh R, Crayford AP, Runyon J, Morris S, Valera-Medina A, Giles A. *Dissociative influence of H_2O vapour/spray on lean blowoff and NOx reduction for heavily carbonaceous syngas swirling flames*. Combust Flame 2017; 177:37–48. ISSN 0010-2180. https://doi.org/10.1016/j.combustflame.2016.11.010.
[19] Baena-Zambrana S, Repetto SL, Lawson CP, Lam JW. *Behaviour of water in jet fuel – a literature review.* Prog Aerosp Sci 2013; 60:35–44. https://doi.org/10.1016/j.paerosci.2012.12.001.
[20] Pourhoseini SH, Yaghoobi M. *Effect of water–kerosene emulsified fuel on radiation, NOx emission and thermal characteristics of a liquid burner flame in lean combustion regime*. J Braz Soc Mech Sci Eng 2018; 40(9):408 (10 pages). DOI:10.1007/s40430-018-1329-8.
[21] Koebel M, Elsener M, Kleemann M. *Urea-SCR: a promising technique to reduce NOx emissions from automotive diesel engines*. Catal Today 2000; 59(3-4):335–45.
[22] Kleemann M, Elsener M, Koebel M, Wokaun A. *Hydrolysis of isocyanic acid on SCR catalysts*. Ind Eng Chem Res 2000; 39(11):4120–6.
[23] Pratt DT. *Performance of ammonia fired gas turbine combustors*. Berkeley (CA): Berkeley University of California, Technical Report No.9, DA-04-200-AMC-791(x); 1967.

[24] Bull MG. *Development of an ammonia-burning gas turbine engine*. San Diego (CA): U.S. Army Engineer Research and Development Laboratories - Solar Turbines International, Technical Report No. ER-1584-3; 1968.
[25] Kobayashi H, Hayakawa A, Somarathne KDK, Okafor A, Ekenechukwu C. *Science and technology of ammonia combustion*. Proc Combust Inst 2019; 37(1):109–33. https://doi.org/10.1016/j.proci.2018.09.029.
[26] http://www.fao.org/fileadmin/templates/AMIS/images/Market_Monitor/fertilizer_prices.pdf.
[27] Mosevitzky B, Azoulay R, Naamat L, Shter GE, Grader GS. *Effects of water content and diluent pressure on the ignition of aqueous ammonia/ammonium nitrate and urea/ammonium nitrate fuels*. Appl Energy 2018; 224:300–8. https://doi.org/10.1016/j.apenergy.2018.04.107.
[28] De Giorgi MG, Fontanarosa D, Ficarella A, Pescini E. *Effects on performance, combustion and pollutants of water emulsified fuel in an aeroengine combustor*. Appl Energy 2020; 260:114263. https://doi.org/10.1016/j.apenergy.2019.114263.
[29] Fontanarosa D, De Giorgi MG, Ciccarella G, Pescini E, Ficarella A. *Combustion performance of a low NOx gas turbine combustor using urea addition into liquid fuel*. Fuel, Volume 288, 2021, 119701, ISSN 0016-2361. https://doi.org/10.1016/j.fuel.2020.119701.